Innovations in Renewable Energies Offshore – Guedes Soares & Wang (Eds)

Exploring dwell time stability in active mechanical motion rectifier based power take-off systems

P. Fornaro
Centre for Ocean Energy Research (COER), National University of Ireland Maynooth, Ireland
Instituto LEICI, Universidad Nacional de La Plata (UNLP) - CONICET, Argentina

P.F. Puleston
Instituto LEICI, Universidad Nacional de La Plata (UNLP) - CONICET, Argentina

J.V. Ringwood
Centre for Ocean Energy Research (COER) National University of Ireland Maynooth, Ireland

ABSTRACT: In wave energy converters (WECs) design, due to the inherently oscillating nature of waves, rectification emerges as an essential requirement. Particularly, active mechanical motion rectification (AMMR) is a novel alternative to include in power take-off systems operating with linear-rotary generators. The primary objective of this mechanism is to ensure controlled unidirectional rotation speed in the generator, aiming to mitigate losses caused by low rotational speed and enhance overall system efficiency. The AMMR operates with a discontinuous switching law to connect and disconnect the WEC body and the generator. Thus, although conceptually simple, the AMMR inclusion significantly increases the complexity of the WEC design. Particularly, ensuring the stability of the system remains an unresolved challenge. To address the latter aspect, in this paper, the AMMR-based WEC is modelled as a switched linear system, assuming a dwell time specification for the switching signals. Then, sufficient and necessary conditions to guarantee closed-loop stability are found. Complementary, provided that the system stability is dependent on both control inputs, the continuous-time electromagnetic torque applied by the generator, and the employed AMMR switching law, stability regions to assess future control development are found, while providing a comprehensive analysis of the (in)stability results.

1 INTRODUCTION

In recent years, extensive research has been conducted to meet the ever-growing energy demand and solve issues related to the availability and mixture of world energy sources. Different non-polluting alternatives have been studied, and particularly, ocean waves have emerged as a promising reservoir of renewable energy, presenting a pivotal opportunity in the quest for a carbon-neutral society. Nonetheless, large-scale implementation of wave energy devices is still economically unfeasible. This is primarily due to the numerous challenges to designing cost-efficient and robust wave energy converters (WECs). In this context, innovation and co-design-based approaches (Garcia-Sanz 2019) (Peña-Sanchez et al. 2022) are essential to address the design problems and limitations that wave energy conversion currently possesses. Irrespective of the employed WEC, the power take-off (PTO) subsystem assumes a pivotal role in converting kinetic energy into electricity (Liu et al. 2020). Among the desired PTO characteristics are high energy conversion efficiency, high system reliability and low maintenance requirements. Therefore, the selection of an appropriate PTO type, along with an associated energy-maximising control algorithm, significantly influences the performance, efficiency, and ultimately, the economic cost of WECs (Ringwood, Zhan, & Faedo 2023). Acknowledging the importance of PTO design, a multitude of PTOs have been developed, each grounded on different concepts (Guo & Ringwood 2021)(Ringwood et al. 2023). The PTO studied in this paper, is a particularly interesting and relatively novel design, termed an active mechanical motion rectifier (AMMR) based PTO. The AMMR (See Figure 1) primary objective is the rectification of mechanical motion. The input shaft of the AMMR is a bi-directional rotational motion and, by a suitable selection of commutation intervals, the output shaft of the AMMR rotates in a single direction. In WECs, the AMMR may be included to prevent the generator from crossing zero velocity. This latter aspect is essential, particularly considering that the low efficiency of linear rotary generators at low speed, reduces the overall WEC wave-to-wire

DOI: 10.1201/9781003558859-36

efficiency (Liang et al. 2017)(Li et al. 2021). Complementary, the AMMR inclusion in the PTO design, brings two important features. Firstly, decoupling between the generator and WEC is possible, allowing the inclusion of a flywheel with the generator, without major impacts on the average harnessed energy (Li et al. 2020)(Yang et al. 2021). Secondly, the mechanical rectification is conducted by connecting and disconnecting two electromagnetic clutches. These clutches may be arbitrarily engaged to connect and disconnect the WCB from the generator, thus, the command signals for the clutches may be regarded as a switching control signal (Fornaro & Ringwood 2024b)(Fornaro & Ringwood 2024a). Consequently, the AMMR inclusion in the PTO design increases the complexity analysis of the AMMR-based WECs and requires the development of specific tools for the analysis and design of dedicated controllers, capable of maximising power output and increasing the overall system efficiency. This novel AMMR-based PTO also brings new engineering challenges to overcome. First, interestingly, most of the existing literature deals with the design of stabilising switching signals, when the closed-loop dynamics of the system are known. However, in the AMMR case, the design of both control inputs (the switching law and the generator torque) may be considered. Second, although in most control applications the reference is known, to maximise the energy extracted from the oscillating waves, a wave excitation force estimate is required (Peña-Sanchez et al. 2019)(Mosquera et al. 2024). This renders the optimal reference time varying and unpredictable. As a result, the stability of the AMMR-based WEC must be guaranteed for a wide range of controller designs.

Because of the switching nature of the AMMR-based PTO, guaranteeing the stability of the closed-loop controlled WEC is not trivial. Thus, before addressing the energy-maximising control design, developing control-oriented methods to analyse the stability of the system in realistic operating conditions is essential. To solve this latter aspect, in this paper, the AMMR-based WEC dynamics are analysed, and tools to guarantee stability in realistic sea realisations, in which the wave resource exhibits a panchromatic behaviour, are provided. The developments introduced in this paper, permit an evaluation of the closed-loop system stability considering a state feedback control and dwell-time specifications for the switching sequences. While the results are focused on low-order controllers, the provided stability conditions are general, and may also be employed for full-order linear controllers analysis. The present work is organised as follows. In section 2, the switched model for the AMMR is developed. In section 3, the tools for the stability analysis of the AMMR-based WEC are developed. Then, in Section 4, illustrative examples are presented. Finally, in Section 5, the paper conclusions are presented.

2 SWITCHED ACTIVE MECHANICAL MOTION RECTIFIER-BASED WEC MODEL

To proceed with the stability analysis of the AMMR-based WEC, developing a complete model, capable of representing the non-linear effects introduced by the AMMR, is required. To that end, it is assumed that the AMMR input may be connected to a variety of wave capture bodies (WCB) (See Figure 1). This permits obtaining general results, which could be easily particularised to different WCBs.

To obtain a complete model for this system, the WCB dynamics, the AMMR, the control structure, and the employed generator must be considered. Thus, in this section, the dynamics of each composing subsystem are presented and discussed.

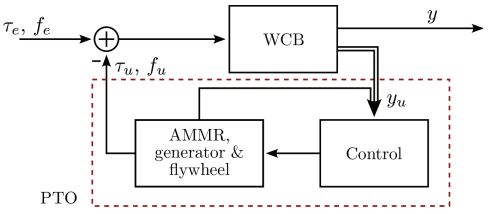

Figure 1. Closed loop structure including the AMMR and generator.

2.1 *Generic wave energy converter linear model*

In this subsection, aiming to develop generic results applicable to a wide variety of wave converters, a generic WCB is assumed. The interested reader may refer to (Yang et al. 2022)(Fornaro & Ringwood 2023) and (Li et al. 2021) for preliminary results obtained employing the AMMR-based PTO with a two-body oscillating point absorber, and an oscillating wave surge converter, respectively.

Regardless of the employed WCB, the input to the AMMR must be a one-degree-of-freedom bi-directional rotational motion. Therefore, for the analysis of the WCB model, a single-degree-of-freedom device is assumed. In this context, the most widespread linear control-oriented model can be represented as:

$$\tilde{J}\ddot{\theta} = \tau_r(\dot{\theta}, \ddot{\theta}) + \tau_k(\theta) + \tau_e + \tau_u, \qquad (1)$$

where θ is angular displacement, $\tilde{J}$ is the WCB inertia, τ_r and τ_k are the radiation and hydrostatic restoring torques that define the free system dynamics, and τ_e and τ_u are the two external forces acting on the body: τ_e is the wave excitation torque, and τ_u is the torque provided by the PTO, which is employed to maximise energy extraction from τ_e. Also, assuming small displacement from an equilibrium position:

$$\tau_k = -k_x \theta, \tag{2}$$

where k_x is the hydrostatic restoring force coefficient. The radiation force may be defined in terms of a non-parametric linear convolution (Cummins 1962):

$$\tau_r = -J_\infty \ddot{\theta} - \underbrace{\int_{t_0}^{t} h_r(t-\varepsilon)\dot{\theta}(\varepsilon)d\varepsilon}_{\tilde{\tau}_r}, \tag{3}$$

where J_∞ is the infinite frequency added-inertia, θ, $\dot{\theta}$, and $\ddot{\theta}$ represent the angular displacement, velocity and acceleration of the WEC, respectively, and h_r is the radiation impulse response kernel. Because of the nature of the system, the convolution operator describes a causal strictly passive system. Additionally, to approximate the convolution from (2), a linear, continuous-time, strictly proper, finite-dimensional system, is considered:

$$\Sigma_r : \begin{cases} \dot{\mathbf{x}}_r &= \mathbf{F}\mathbf{x}_r + \mathbf{G}\dot{\theta}, & (4a) \\ \tilde{\tau}_r &\approx \mathbf{H}\mathbf{x}_r, & (4b) \end{cases}$$

with $\mathbf{F} \in \mathbb{R}^{n_r \times n_r}$ Hurwitz, and $\mathbf{G} \in \mathbb{R}^{n_r \times 1}$ and $\mathbf{H} \in \mathbb{R}^{1 \times n_r}$. Thus, $\mathbf{x}_r^\top = [x_{r_1}, \ldots, x_{n_r}]$. For further discussion on Σ_r, see (Pérez & Fossen 2008).

2.2 *AMMR model*

A simplified schematic of the AMMR gearbox is illustrated in Figure 2, where the three AMMR operation modes can be appreciated. To refer to the different operation modes, the notation $q \in \mathcal{Q} : \{-1, 0, 1\}$ is employed. With $q = 1$ the positive clutch is engaged, with $q = -1$ the negative clutch is engaged and, with $q = 0$ the clutches are disengaged.

During normal operation, the AMMR engages and disengages the generator and flywheel from the WCB. Thus, the transient response of the generator and flywheel must be considered in the model. To model the AMMR transient response, firstly, the losses are considered utilising a constant k_b. Secondly, a spring constant k_s is included to model torsional effects on the AMMR gears. Complementary, the generator and flywheel losses are included in k_b. Thus, the generator and AMMR dynamics are:

$$J_g \ddot{\theta}_g = q(\tau_l + \tau_s) + q\,\tau_{em} - (1 - |q|)k_d \dot{\theta}_g, \tag{5a}$$

$$\tau_u = -(\tau_s + \tau_l), \tag{5b}$$

$$\tau_l = q\,k_b(q\dot{\theta} - \dot{\theta}_g) \tag{5c}$$

$$\dot{\tau}_s = q\,k_s(q\dot{\theta} - \dot{\theta}_g), \tag{5d}$$

where $\dot{\theta}_g$ and $\ddot{\theta}_g$ are the generator velocity and acceleration respectively, J_g lumps the generator and flywheel inertia, and τ_{em} represents the electromagnetic torque, applied to control the WCB using a continuous control action. τ_l represents the AMMR friction torque, τ_s the AMMR stiffness torque, $q \in \mathcal{Q} : \{-1, 1, 0\}$ are the discrete states of the switching signal $\sigma(t)$.

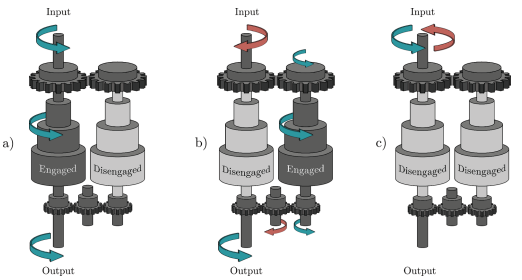

Figure 2. Illustrative AMMR in operation. a) Direct coupling (Engaging the positive clutch). b) Indirect coupling (Engaging the negative clutch). c) Declutching the AMMR. In this scenario, the input and the output are decoupled.

2.3 *Full switched linear WEC model*

In this subsection, the switched model of the AMMR-based WEC is formulated. Considering equations (1) to (5), and the dependence on the discrete states q, the complete open-loop model of the AMMR-based WEC results:

$$\Sigma_W : \begin{cases} \dot{\mathbf{x}} &= \mathbf{A}_q \mathbf{x} + \mathbf{B}_q \begin{bmatrix} \tau_{ex} \\ \tau_{em} \end{bmatrix}, & (6a) \\ \mathbf{y}_u &= \mathbf{C}_q \mathbf{x} + [\,\mathbf{D}_q \quad 0\,] \begin{bmatrix} \tau_{ex} \\ \tau_{em} \end{bmatrix}, & (6b) \\ y &= [\,0 \quad 1 \quad \mathbf{0} \quad 0 \quad 0\,]\mathbf{x}, & (6c) \end{cases}$$

where $\mathbf{x} \in \mathbb{R}^n$ is $\mathbf{x} = [\theta\dot{\theta}\,\mathbf{x}_r^T\,\dot{\theta}_g\tau_s]$, and with:

$$A_q = \begin{bmatrix} 0 & 1 & \mathbf{0} & 0 & 0 \\ \frac{-k_x}{J} & -\frac{|q|k_b}{J} & -\frac{\mathbf{H}}{J} & \frac{q k_b}{J} & \frac{-1}{J} \\ \mathbf{0} & \mathbf{G} & \mathbf{F} & \mathbf{0} & \mathbf{0} \\ 0 & \frac{q\,k_b}{J_g} & \mathbf{0} & \frac{-|q|k_b - (1-|q|)k_d}{J_g} & \frac{q}{J_g} \\ 0 & |q|k_s & \mathbf{0} & -q\,k_s & 0 \end{bmatrix}, \tag{7}$$

$$B_q^T = \begin{bmatrix} 0 & \frac{1}{J} & \mathbf{0} & 0 & 0 \\ 0 & 0 & \mathbf{0} & \frac{q}{J_g} & 0 \end{bmatrix}, \tag{8}$$

$$C_q = \begin{bmatrix} 1 & 0 & \mathbf{0} & 0 & 0 \\ 0 & 1 & \mathbf{0} & 0 & 0 \\ 0 & 0 & \mathbf{0} & 1 & 0 \end{bmatrix}, \quad D_q = [\mathbf{0}], \quad (9)$$

with the zero vectors and matrices taking the appropriate dimensions. Also, τ_{em} is the control action to be designed employing the control output $\mathbf{y}_u$ and $J = \tilde{J} + J_\infty$. Although the system dynamics change for the different values of q, the states $\mathbf{x}$ are continuous, while the control action τ_{em} may be discontinuous. It should be also noted that, although $\mathbf{D}_q = 0$ is generally the case, $\mathbf{y}$ is assumed to be a generic output employed for control design. Thus, $\mathbf{C}_q \in \mathbb{R}^{n_p \times n}$, and $\mathbf{D}_q \in \mathbb{R}^{n_p \times 1}$, with $n_p = 3$ being the order of the output employed for control design, assuming that the output consists of WCB position, velocity, and generator angular velocity. It is worth noting that, the second term in the direct transfer term matrix is zero without loss of generality.

3 STABILITY ANALYSIS FOR THE AMMR

Due to the inherent switching structure, guaranteeing the stability of the AMMR-based WEC is not trivial (Shorten et al. 2007). Thus, in this paper, the main goal is to analyse the stability of the WEC switched system, assuming different operating conditions for both the switching law and controller structure. Specifically, is assumed:

• A time constraint for the switching signals, typically referred to as *dwell time* specification. This indicates that the switching signal $\sigma(t) = q \in \mathcal{Q} : \{-1, 0, 1\}, \quad \forall t \in [t_k, t_{k+1})$ with $t_{k+1} - t_k \geq T^\star$. $T^\star$ is called the application dwell time, and the switching signals that satisfy this condition are concisely written as: $\sigma(t) \in \mathcal{D}_{T^\star}$

• A pure state feedback controller. In accordance with (9), the controlled variables are θ, $\dot{\theta}$ and $\dot{\theta}_g$.

• Only two states for the switching signal are considered, provided that, the AMMR only *connects* or *disconnects* the WCB from the generator. Thus $\sigma(t) = q \in \mathcal{Q} : \{0, 1\}$.

Formally, throughout this paper, the switched model adopted for the stability analysis is a closed loop structure, which implicitly includes the controller structure:

$$\Sigma_S : \begin{cases} \dot{\mathbf{x}} &= \mathcal{A}_{\sigma(t)}\mathbf{x} + \mathcal{B}_{\sigma(t)}\tau_e, & (10a) \\ y &= \mathcal{C}_{\sigma(t)}\mathbf{x}. & (10b) \end{cases}$$

where $\mathcal{A}_{\sigma(t)}$, $\mathcal{C}_{\sigma(t)}$ and $\mathcal{B}_{\sigma(t)}$, represent closed-loop matrices of the controlled switched system, and the switching function $\sigma(t) : \mathbb{R}^+ \to \{0, 1\}$ satisfies the dwell time specification. The discontinuity points in $\sigma(t)$, are known as switching instances. Because a pure state feedback controller is assumed, the triple that defines (10) is:

$$\mathcal{A}_{\sigma(t)} = \mathbf{A}_q + \mathbf{K}\mathbf{B}_q, \quad (11a)$$

$$\mathcal{B}^{\mathrm{T}}_{\sigma(t)} = \begin{bmatrix} 0 & \frac{1}{J} & \mathbf{0} & 0 & 0 \end{bmatrix}, \quad (11b)$$

$$\mathcal{C}_{\sigma(t)} = [0 \quad 1 \quad \mathbf{0} \quad 0 \quad 0], \quad (11c)$$

3.1 *Dwell time stability conditions*

Since the stability of (10) is independent of τ_e, the stability of $\dot{\mathbf{x}} = \mathcal{A}_{\sigma(t)}\mathbf{x}$ is analysed, considering, without loss of generality, that $\tau_e = 0$. Then, the following linear matrix inequality (LMI) condition is derived from the developments in (Geromel & Colaneri 2006):

$$\begin{bmatrix} A_i^{\top_i} + Z_i A_i + \hat{Q}_i & Z_i B_i - \hat{S}_i \\ \star & -\hat{R}_i \end{bmatrix} < 0, \quad (12a)$$

$$e^{A_i^\top T} Z_j e^{A_i T} - Z_i + P_i(T) < 0, \quad (12b)$$

which are built assuming positive constants (Q, S, R), and defining:

$$\hat{Q}_i = C_i^\top Q C_i, \quad (13a)$$

$$\hat{S}_i = C_i^\top S + C_i^\top Q D_i, \quad (13b)$$

$$\hat{R}_i = D_i^\top Q D_i + D_i^\top S + S^\top D_i + R, \quad (13c)$$

$$P_i(T) = P_i^\star - e^{H_i^\top} P_i^\star e^{H_i \top_T}, \quad (13d)$$

$$H_i = A_i + B_i \hat{R}_i^{-1}(B_i^\top P_i^\star - \hat{S}_i), \quad (13e)$$

and $P_i^\star$ being the (infinite horizon) stabilising solution of the algebraic Ricatti equation associated with (14):

$$0 = A_i^\top P_i^\star + P_i^\star A_i + (P_i^\star B_i - \widehat{S}_i)\widehat{R}_i^{-1}(P_i^\star B_i - \widehat{S}_i)^\top. \quad (14)$$

If conditions (12) hold, then system (6) is dissipative for switching signals $\sigma(t) \in \mathcal{D}_T$. However, the LMI (12) does not provide information on the effects that cause the system instability. Thus, the proposal presented in this paper consists of recursively evaluating (12) for different controller gains. Additionally, because dissipative systems with positive Q, R, S are also very strictly passive (For further details please refer to (Kottenstette et al. 2014)), the analysis can be conducted without including the radiation dynamics in the system, alleviating the computational burden. This is because the radiation dynamics are also passive, and

feedback interconnection of passive systems does not modify the closed-loop passivity of the system.

As illustrated in the results (Section 4), the instability is created by differences in the transient response of the system. However, it is also dependent on the selected T. Thus, the first required step is obtaining a realistic application dwell time $T^\star$.

3.2 *Bounds for the application dwell time*

The AMMR-based WEC application dwell time depends on two different effects. The first one is the physical limitation of the AMMR electromagnetic clutches. In (Yang, Huang, Congpuong, Chen, Mi, Bacelli, & Zuo 2021), it is stated that the AMMR cannot be connected or disconnected at a rate higher than 0.1s. The second one, however, is obtained from considerations for a realistic application scenario. Since the AMMR primary function is to rectify the WCB velocity, four connections per period of the wave excitation force are expected. Therefore, an approximation of the minimum required switching time would be $T^\star \geq 2\pi/(\omega^\star 5)$, with $\omega^\star$ being an upper bound for energetic waves in a particular sea state.

In the following section, to illustrate the impact of the dwell time selection for the stability analysis, results considering different times T are shown.

4 NUMERICAL EXAMPLE

To perform a preliminary evaluation of the proposed methodology, the AMMR is assumed to operate with a heaving point absorber buoy (Mosquera, Fornaro, Puleston, & evangelista John V. Ringwood 2024), with parameters as presented in Table 1. This is a one-degree-of-freedom device, which satisfies (1). Then, employing the conditions from Section 3, the stability regions are computed evaluating (12) for different values of $T^\star$, and locations for the closed-loop poles of the controlled system (i.e., when $q = \pm 1$). Employing the conditions from Table 1, the triple from system, employed for the stability analysis (6) reads as:

$$A_q = \begin{bmatrix} 0 & 1 & 0 \\ \frac{-k_s}{J} & -\frac{|q|k_b}{J} & \frac{qk_b}{J} \\ 0 & \frac{qk_b}{J_g} & \frac{-|q|k_b-(1-|q|)k_d}{J_g} \end{bmatrix}, \tag{15a}$$

$$\mathrm{B}_q^\top = \begin{bmatrix} 0 & \frac{1}{J} & 0 \\ 0 & 0 & \frac{q}{J_g} \end{bmatrix}, \tag{15b}$$

$$C_q = \begin{bmatrix} 1 & 0 & 0 \\ 0 & 1 & 0 \\ 0 & 0 & 1 \end{bmatrix}, \quad D_q = [\mathbf{0}]. \tag{15c}$$

Also, in this section, condition (12) is analysed with $Q = 0$, $R = 1$ and $S = 1/2$, for which every (A_q, B_q, C_q) must be strictly output passive. It is worth noting that if the dissipativity condition (12) is satisfied, then the system that includes the radiation dynamics is also stable. This is because as mentioned in Section 3, the radiation subsystem is also passive, thus, in this section, is not included.

In the following Subsections, the cases with $T^\star \to 0$ and $T^\star \neq 0$ are separately analysed. Regarding the controller parameters, it is assumed that the gain $\mathbf{K} = [k_1\, k_2\, k_3]$ is employed, where k_1 and k_2 are the feedback gains employed to control the WEC position and velocity respectively, and k_3 controls the generator velocity.

The stability region depends on the selection of the gain $\mathbf{K}$ and, the transient response of the system is not only affected by the WCB dominant poles but also by the generator dynamics. Thus, as k_3 is modified, the stability region also changes. This latter aspect is essential, not only for the design of the control but also for the design of the system itself, provided the generator inertia and other AMMR parameters define the dynamics of the faster eigenvalue of the system. Considering the latter aspects, in this preliminary analysis, it is assumed that the system dominant eigenvalues correspond to the WCB structure. Therefore, the gain k_3 is assumed constant, and the effects of controlling the dominant poles of the system are analysed by varying k_2 and k_3.

Table 1. Nominal AMMR system model employed for stability assessment.

AMMR and WEC parameters					
	Kgm^2		Nm/rad		N.A.
J	$1,46.10^5$	k_z	$5,57.10^5$	n_r	7
J_g	$1,46.10^4$	k_b	5.10^5	k_s	0

4.1 *Arbitrary switching*

As mentioned in Section 3, to guarantee the passivity of the switched system, the radiation dynamics are not contemplated. Considering this latter aspect, the eigenvalues of the uncontrolled reduced system, with $q = 0$, are presented in Figure 1, together with the eigenvalues of the discrete state $q = 1$ for different values of k_1 and k_2. Intuitively, if the poles of the controlled system ($q = 1$) are close to the poles with $q = 0$, the system should remain passive, even considering $T^\star \to 0$. This latter case is termed the *arbitrary switching* case.

In Figure 1, the stability region for the arbitrary switching case is depicted, considering $k_3 = -200$, variable gains k_1 and k_2, and $T = 0.001s$. It can be appreciated that the stability region resembles a semicircle with a constant radius, determined by the imaginary part of the eigenvalues with $q = 0$, in accordance with preliminary theoretical results (Shorten et al. 2007).

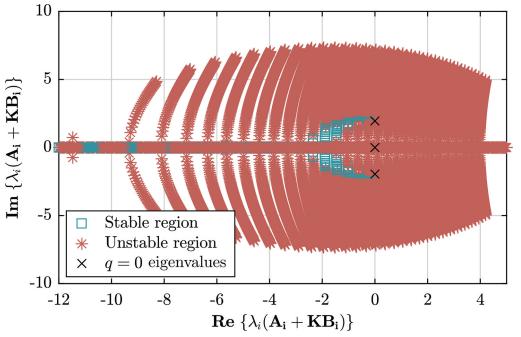

Figure 3. Stable and unstable regions for $T = 0.001$.

4.2 *Dwell-time specification*

This subsection analyses the case with $T^\star > 0$. A first remark is that, while a dwell time specification is a more relaxed condition for the stability of switched systems, finding a suitable bound for the minimum dwell time for a specific system is a challenging task. Indeed, the stability constraints (12) represent a conservative case (Geromel & Colaneri 2006) and, in practice, the stability region may not be precise.

Considering the mentioned aspects, to evaluate the effects of different T, three different scenarios were simulated, with $T = [0.3,\ 0.4,\ 0.5,\ 2]$, $k_3 = -200$ and varying k_1 and k_2. From Figures 4 to 6 can be appreciated how increasing the considered dwell time also increases the stability region. As larger values for T are considered, it can be appreciated how the stability region increases from the arbitrary switching case.

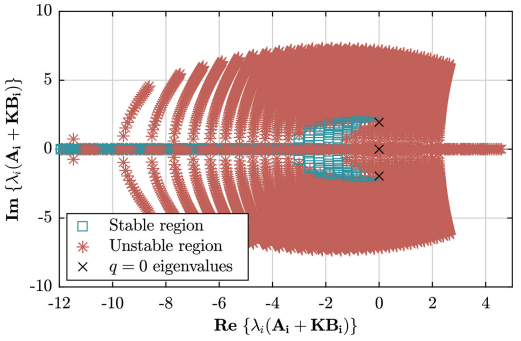

Figure 4. Stable and unstable regions with $T = 0.3s$.

Regardless of the different results, there is a common aspect to all three scenarios: When the closed loop poles are too close to the origin, the system becomes unstable. This phenomenon is associated with the fact that a slow transient response also represents a slow energy-rate decay and, thus, only with a slower switching dwell time the system could preserve the dissipativity rate constraint defined in (12).

Regarding the obtained results, the following additional remarks are made. First, obtaining an

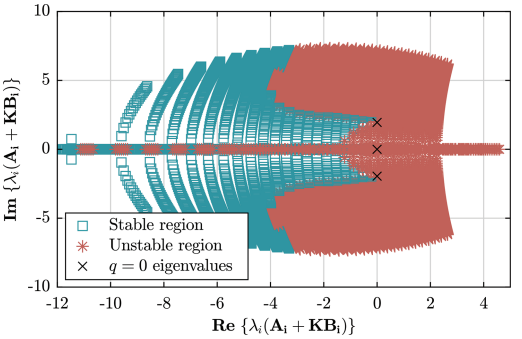

Figure 5. Stable and unstable regions with $T = 0.4s$.

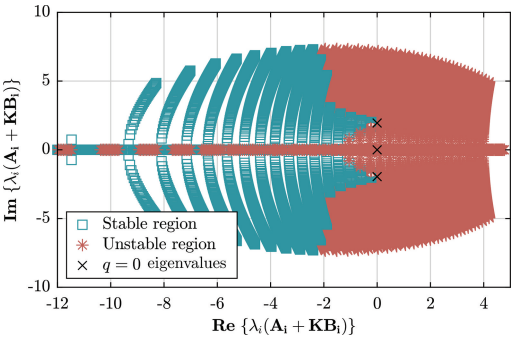

Figure 6. Stable and unstable regions with $T = 0.5s$.

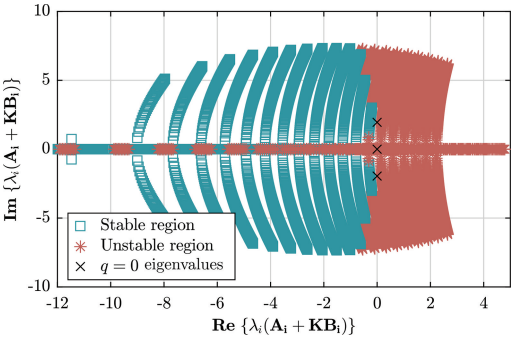

Figure 7. Stable and unstable regions with $T = 2s$.

analytical result for the presented bounds has eluded the community for systems with order higher than 2 (Shorten et al. 2007). Thus, the presented results are focused in an area close to the origin, where solutions hold practical significance. For the same reason, the real axis is not analysed, considering it lacks practical relevance in the context of wave energy applications.

5 CONCLUSIONS

In this paper, the stability of a WEC operating with an AMMR was analysed. Employing mechanical

rectification, the system becomes switched and, since wave energy devices are inherently oscillating systems, instability arises as a natural result. However, the stability depends not only on the controller parameters but also on the system dynamical characteristics, and on the specified dwell time condition for the switching law. In this context, the analysis of AMMR-based WECs stability plays an essential role to address, in the future, the design of energy-maximising controllers for these systems.

To obtain stability regions for the AMMR-based WEC, the AMMR dynamics were included in the model, also modelling the WCB as a linear system. Then, assuming a state feedback controller, an LMI stability condition was formulated. This condition depends not only on the controller gains but also on the specified dwell time. Thus, considering a set of dwell time specifications, and gains for the state feedback controller, stability regions for the design of stable controllers were found, proving that increasing dwell time enhances the overall AMMR-based WEC stability and laying the foundations for future hybrid control design.

The presented method to analyse the stability of the switched system is versatile and of simple implementation. Also, permits the evaluation of the stability of different controller structures. Furthermore, it is also generic, since the stability results are independent of the considered radiation dynamics. The extension of the results for other controller structures, and of the LMI formulation, remain to be addressed in future work.

ACKNOWLEDGEMENTS

This work was possible thanks to the support of the National University of Maynooth, Science Foundation Ireland under grant number 21/US/3776, and of the University Nacional de La Plata, CONICET and ANCyT, Argentina.

REFERENCES

Cummins, W. E. (1962). The impulse response function and ship motions. Technical report,.

Fornaro, P. & J. V. Ringwood (2023). Stability analysis of an active mechanical motion rectifier for wave energy conversion systems. In *XX Workshop on signal processing and control - RPIC*.

Fornaro, P. & J. V. Ringwood (2024a). Hybrid optimal control for an active mechanical motion rectifier for wave energy converters via separation principle. In *2024 European Control Conference*, *Stockholm, Sweden*.

Fornaro, P. & J. V. Ringwood (2024b). On the controllability of an active mechanical motion rectifier for wave energy converters. In *2024 American Control Conference*, *Toronto, Canada*.

Garcia-Sanz, M. (2019). Control co-design: An engineering game changer. *Advanced Control for Applications 1*(1), .

Geromel, J. C. & P. Colaneri (2006). Stability and stabilization of continuous-time switched linear systems. *SIAM Journal on Control and Optimization 45*(5), 1915–1930.

Guo, B. & J. V. Ringwood (2021). A review of wave energy technology from a research and commercial perspective. *IET Renewable Power Generation 15*(14), 3065–3090.

Kottenstette, N., M. J. McCourt, M. Xia, V. Gupta, & P. J. Antsaklis (2014). On relationships among passivity, positive realness, and dissipativity in linear systems. *Automatica 50*(4), 1003–1016.

Li, X., C. Chen, Q. Li, L. Xu, C. Liang, K. Ngo, R. G. Parker, & L. Zuo (2020). A compact mechanical PTO for wave energy converters: Design, analysis, and test verification. *Ap. Energy 278*, .

Li, X., D. Martin, C. Liang, C. Chen, R. G. Parker, & L. Zuo (2021). Characterization and verification of a two-body wave energy converter with a novel PTO. *Renewable Energy 163*, 910–920.

Liang, C., J. Ai, & L. Zuo (2017). Design, fabrication, simulation and testing of an ocean wave energy converter with mechanical motion rectifier. *Ocean Engineering 136*, 190–200.

Liu, Z., R. Zhang, H. Xiao, & X. Wang (2020). Survey of the mechanisms of power take-off (pto) devices of wave energy converters. *Acta Mechanica Sinica 36*(3), 644–658.

Mosquera, F., P. Fornaro, P. Puleston, & C. evangelista John V. Ringwood (2024). A sliding mode-based tracking observer for excitation force estimation in wave energy systems. In *8 IEEE conference on control technology and applications*.

Peña-Sanchez, Y., D. Garca-Violini, & J. V. Ringwood (2022). Control co-design of power take-off parameters for wave energy systems. *IFAC-PapersOnLine 55*(27), 311–316.

Peña-Sanchez, Y., C. Windt, J. Davidson, & J. V. Ringwood (2019, November). A critical comparison of excitation force estimators for wave-energy devices. *IEEE Trans. Control Syst. Technol. 28*(6), .

Pérez, T. & T. I. Fossen (2008). Time-vs. frequency-domain identification of parametric radiation force models for marine structures at zero speed. *Model. Identif. Control 29*(1), 1–19.

Ringwood, J. V., S. Zhan, & N. Faedo (2023). Empowering wave energy with control technology: Possibilities and pitfalls. *Annual Reviews in Control 55*, 18–44.

Shorten, R., F. Wirth, O. Mason, K. Wulff, & C. King (2007). Stability criteria for switched and hybrid systems. *SIAM Review 49*(4), 545–592.

Yang, L., J. Huang, N. Congpuong, S. Chen, J. Mi, G. Bacelli, & L. Zuo (2021). Control co-design and characterization of a power takeoff for wave energy conversion based on active mechanical motion rectification. *IFAC-PapersOnLine 54*(20), 198–203.

Yang, L., J. Huang, J. Mi, M. Hajj, G. Bacelli, & L. Zuo (2022). Optimal power analysis of a wave energy converter with a controllable power takeoff based on active motion rectification. *IFAC-PapersOnLine 55*(27), 299–304.